Received: 23 January 2021 | Revised: 16 May 2021 | Accepted: 18 May 2021

DOI: 10.1111/pce.14117

ORIGINAL ARTICLE

Plant, Cell & Environment WILEY

Manipulating phloem transport affects wood formation but not local nonstructural carbon reserves in an evergreen conifer

Tim Rademacher[1,2,3] | Patrick Fonti[4] | James M. LeMoine[1,2] | Marina V. Fonti[4,5] | David Basler[3] | Yizhao Chen[6] | Andrew D. Friend[6] | Bijan Seyednasrollah[1,2] | Annemarie H. Eckes-Shephard[6] | Andrew D. Richardson[1,2]

[1]School of Informatics, Computing, and Cyber Security, Northern Arizona University, Flagstaff, Arizona

[2]Center for Ecosystem Science and Society, Northern Arizona University, Flagstaff, Arizona

[3]Department of Organismic and Evolutionary Biology, Harvard University, Cambridge, Massachusetts

[4]Swiss Federal Research Institute for Forest, Snow and Landscape Research WSL, Birmensdorf, Switzerland

[5]Institute of Ecology and Geography, Siberian Federal University, Krasnoyarsk, Russian Federation

[6]Department of Geography, University of Cambridge, Cambridge, UK

Correspondence
Tim Rademacher, School of Informatics, Computing, and Cyber Security, Northern Arizona University, Flagstaff, AZ, USA.
Email: trademacher@fas.harvard.edu

Funding information
National Science Foundation, Grant/Award Numbers: DEB- 1741585, DEB-1237491, DEB-1832210; Natural Environment Research Council, Grant/Award Number: NE/P011462/1; Schweizerischer Nationalfonds zur Förderung der Wissenschaftlichen Forschung, Grant/Award Number: PSBSP3-168701

Abstract

How variations in carbon supply affect wood formation remains poorly understood in particular in mature forest trees. To elucidate how carbon supply affects carbon allocation and wood formation, we attempted to manipulate carbon supply to the cambial region by phloem girdling and compression during the mid- and late-growing season and measured effects on structural development, CO_2 efflux and nonstructural carbon reserves in stems of mature white pines. Wood formation and stem CO_2 efflux varied with a location relative to treatment (i.e., above or below the restriction). We observed up to twice as many tracheids formed above versus below the treatment after the phloem transport manipulation, whereas the cell-wall area decreased only slightly below the treatments, and cell size did not change relative to the control. Nonstructural carbon reserves in the xylem, needles and roots were largely unaffected by the treatments. Our results suggest that low and high carbon supply affects wood formation, primarily through a strong effect on cell proliferation, and respiration, but local nonstructural carbon concentrations appear to be maintained homeostatically. This contrasts with reports of decoupling of source activity and wood formation at the whole-tree or ecosystem level, highlighting the need to better understand organ-specific responses, within-tree feedbacks, as well as phenological and ontogenetic effects on sink-source dynamics.

KEYWORDS
allocation, girdling, growth, *Pinus strobus*, respiration, wood anatomy, xylogenesis

1 | INTRODUCTION

Forests sequester about 14% of anthropogenic carbon emissions each year providing a crucial global mitigation service in the face of climate change (Pan et al., 2011). Since wood has a long turnover time and is composed of roughly 50% carbon (Lamlom & Savidge, 2003), allocation to wood is an important part of the land carbon sink (Pugh, Rademacher, Shafer, et al., 2020). Understanding the mechanisms of carbon allocation to wood formation is, therefore, crucial to assess land carbon sequestration in a rapidly changing world (Hartmann, Bahn, Carbone, & Richardson, 2020) and for accurate predictions of the land carbon cycle (Friend et al., 2019). Yet, what controls carbon allocation to wood formation is an unsettled debate (Gessler & Grossiord, 2019). On the one hand, source activity controls carbon allocation to woody tissues in most models (Friend et al., 2014; Galbraith et al., 2013). On the other hand, experimental evidence for whole trees suggests that sink activity is more often limiting than source activity (Cabon, Peters, Fonti, Martínez-Vilalta, &

Cáceres, 2020; Fatichi, Leuzinger, & Körner, 2014; Vieira, Carvalho, & Campelo, 2020), especially in mature trees (Körner et al., 2005). To disentangle the complex and dynamic physiological feedbacks regulating source and sink dynamics at the whole-tree scale (Salmon et al., 2020; Walker, Kauwe, Bastos, et al., 2021), we require a fundamental understanding of the effects of variations in carbon supply on allocation to wood formation in the cambial region of mature trees. Understanding under what circumstances carbon supply or demand control wood formation, thus long-term forest carbon sequestration, is crucial to improve our assessment of forests' mitigation potential under climate change.

At the tree and ecosystem level, many studies have focused on assessing the "fate" of assimilated carbon in land plants (Atkin, 2015), highlighting the dynamic relationship between sources, sinks and storage, but less is known about the responses in wood forming tissues. We do know that nonstructural carbon reserves in woody tissue constitute the majority of total tree carbon reserves (Furze et al., 2019) and isotopic evidence suggests that local reserves can be tapped into when phloem transport is limited following girdling (Maunoury-Danger et al., 2010; Muhr, Trumbore, Higuchi, & Kunert, 2018). Indeed, stem starch concentrations can increase above a girdle and decrease below (Jordan & Habib, 1996; Moscatello et al., 2017), although in some cases stem concentrations do not change clearly (Maier, Johnsen, Clinton, & Ludovici, 2010), or only distal reserves in the roots are depleted (Regier, Streb, Zeeman, & Frey, 2010). But if even decade-old local carbon (Carbone et al., 2013; Muhr et al., 2018; Vargas, Trumbore, & Allen, 2009) can be remobilized to fuel growth and metabolism, it is not clear whether the small observed change in local reserves suffices to fuel the seemingly larger changes in growth and respiration following phloem transport manipulations, such as phloem chilling (De Schepper, Vanhaecke, & Steppe, 2011), compression (Henriksson et al., 2015) and girdling (Daudet, 2004; Domec & Pruyn, 2008; Maier et al., 2010; Maunoury-Danger et al., 2010; Wilson, 1968; Winkler & Oberhuber, 2017). To the best of our knowledge, no study has attempted to link a quantitative response of carbon allocation in the stems of mature trees to variations in carbon supply, despite the fundamental importance of a wood forming tissue perspective to disentangle source-sink dynamics within trees.

Wood formation can be divided into several constituent and overlapping processes, but how each of these processes responds to carbon supply variations also remains untested in large trees. Each new xylem cell starts by dividing from a cambial mother cell, goes through enlarging, cell-wall thickening and cell-wall lignification before it dies to become part of the functioning xylem (Rathgeber, Cuny, & Fonti, 2016). Conifers in habitats with seasonal growth limitations (e.g., cold or dry) seem to obey tight developmental programmes that feature regular transitions in cell characteristics within each growth ring, from large thin-walled tracheids early in the season to smaller, thicker-walled latewood cells (Cuny & Rathgeber, 2016). Sugar concentrations in the cambium are known to partially generate the turgor necessary for cambial cell division and cell enlargement (Boyer, 1968; Gould et al., 1977; Hsiao et al., 1976; Peters et al., 2021) and provide a direct signal-regulating cell division (Lastdrager, Hanson, & Smeekens, 2014; Riou-Khamlichi, Menges, Healy, & Murray, 2000; Smith & Stitt, 2007). Moreover, cambial sugar concentrations have been argued to drive the intra-annual transition in wood characteristics (Cartenì et al., 2018). As a result of these multiple roles of cambial sugar concentrations, carbon supply variations would be expected to affect the number of cells, their sizes and cell-wall areas. The one study that explored the effects of carbon supply variation on wood anatomy in Norway spruce saplings showed that carbon supply did positively relate to the number of cells formed and lumen diameter, but negatively to cell-wall thickness in latewood (Winkler & Oberhuber, 2017). Defoliation studies support the positive relation of carbon supply with cell numbers, but showed no clear effect of reduced carbon supply on cell size and/or cell-wall deposition (Castagneri et al., 2020; Deslauriers, Caron, & Rossi, 2015; Rossi, Simard, Deslauriers, & Morin, 2009), suggesting that the primary effect of carbon supply is on cell numbers. As cell-wall density is fairly constant (Björklund et al., 2017), the amount of carbon in a growth ring depends primarily on its cumulative cell-wall area, hence the number of cells and individual cell-wall areas. In contrast, the ring's width is a function of the number of cells and their size (e.g., radial lumen diameter and tangential cell-wall thickness). If carbon supply variations mainly affect cell numbers, future ring width under increased atmospheric CO_2 and carbon supply would be expected to be proportionately larger. However, if these rings will sequester proportional amounts of carbon, will be determined by whether cell-wall deposition decreases (as indicated by Winkler & Oberhuber, 2017) or not (as indicated by above-mentioned defoliation studies). Consequently, understanding the effects of carbon supply variation on the number of xylem cells, their size and cell-wall area in mature trees, is crucial to project future changes in volume and mass growth.

When focusing solely on local carbon pools and fluxes relevant to wood growth (e.g., respiration, structural carbon and nonstructural carbon) in wood forming tissues, we can use phloem transport manipulations to vary local carbon supply in stems of mature forest trees. While most manipulation experiments are conducted on seedlings or saplings, phloem transport manipulations can provide a rare perspective to better understand local responses to carbon supply variations of mature forest trees. Indeed, evidence from tree rings of naturally growing trees suggests a declining response of radial growth to increasing CO_2 with age (Voelker, Muzika, Guyette, & Stambaugh, 2006; Walker et al., 2021) or no response at all (van der Sleen et al., 2015), which has also been corroborated in one CO_2 enrichment study on mature trees (Körner et al., 2005). Generally, smaller trees may be more carbon-limited (Hayat, Hacket-Pain, Pretzsch, Rademacher, & Friend, 2017; Körner, 2003) due to ontogenetic differences in carbon allocation (Hartmann et al., 2018), which could explain discrepancies in growth response between smaller and larger trees and warrants extreme caution when extrapolating results from experiments on potted saplings to forest trees. In addition to the ability to perform direct phloem transport manipulations on mature trees, these restrictions can generate a large contrast in local carbon supply without affecting light, temperature, water availability or nutrient availability for the whole tree (for a recent review see Rademacher

et al., 2019), reducing the potential for confounding environmental factors (e.g., temperature, water status and light environment) influencing wood formation (Begum, Kudo, Rahman, et al., 2018; Cabon, Peters, et al., 2020; Steppe, Sterck, & Deslauriers, 2015). Thus, phloem transport manipulations can provide insight into carbon allocation by varying carbon supply to wood formation in mature forest trees.

The objective of our study is to investigate how carbon supply controls wood formation in stems of mature trees during high carbon demand under similar environmental and phenological conditions. We applied phloem girdling and compression to restrict carbon flow along the stem by cutting or exerting theoretically sufficient pressure to collapse phloem tissues around the stem (Henriksson & Rademacher, 2019). To test whether local carbon dynamics change, when a stem section is isolated from both canopy carbon supply and distal nonstructural carbon reserves (i.e., roots), we also included a double compression treatment. The resulting carbon-supply gradient is presumed to range from severe carbon limitation below the girdle, over moderate carbon limitation below the compressions (due to some leakage), through moderate carbon supply surplus above the compression, to a larger surplus above the girdle.

Mass growth in conifers peaks about a month after volume growth (Cuny et al., 2015), which peaks around the summer solstice in seasonally limited habitats (Rossi et al., 2006). Consequently, focussing on the mid- to late-growing season, when mass growth peaks, allowed us to investigate the role of carbon supply in the intra-annual transition to latewood without the risk of causing the complete halt of radial growth (e.g., missing ring) due to the lack of carbon supply during the resumption of cambial activity in the early growing season. Previous phloem transport manipulations produced the largest effects when applied in the mid- to late-growing season (De Schepper et al., 2011; Maier et al., 2010), further justifying a start date in the mid-growing season. Through these induced gradients in carbon supply along the stems of mature forest trees, we investigated the overarching question of how carbon allocation between growth, stem CO_2 efflux and nonstructural carbon reserves vary with carbon supply. Assuming that local carbon sinks are mainly supply-limited (as shown in previous phloem transport manipulations), we hypothesized that (H1), that the ratios of carbon allocated to newly formed structural carbon, local bulk nonstructural carbon reserves and CO_2 efflux would be constant across the presumed gradient of carbon supply in the stem of mature white pines. Based on previous studies that showed changes in cell numbers and cell-wall thicknesses with carbon status (Castagneri et al., 2020; Deslauriers et al., 2015; Rossi et al., 2009; Winkler & Oberhuber, 2017), we expected that absolute differences in structural carbon growth, resulting from differences in carbon supply, would be driven by underlying changes in both (H2) cell numbers and (H3) average cell-wall area per cell with (H4) no clear differences in cell size with carbon supply. By testing these hypotheses, we expect to be able to answer the fundamental question of whether carbon allocation to wood forming tissues, including to individual wood formation processes, is generally limited by carbon supply in mature forest trees.

2 | MATERIALS AND METHODS

2.1 | Study site

Harvard Forest is a mesic temperate mixed forest dominated by oak, maple and pine species located in central Massachusetts, USA. Soils at Harvard Forest are derived from glacial till and characterized as well-draining, slightly acidic sandy loam with an average depth of 1 m. Mean annual temperature at the site is 8.0 ± 0.8°C ($\mu \pm \sigma$) and mean total annual precipitation is 1170 ± 193 mm, evenly spread across all seasons (Boose & Gould, 2019).

The experiment was conducted on an even-aged cohort of white pines (*Pinus strobus* L.) with homogenous growing conditions. The stand is located at 42°30.8′N and 72°13.1′W, 340 m above sea level, and has been naturally regenerating since a 1990 harvest of red pine (*Pinus resinosa* Ait.) plantation. Spacing was dense at circa. 1600 trees per hectare. For the experiment, we selected 40, healthy, single-stemmed, co-dominant white pines. At the beginning of the experiment, the selected trees were on average 18 ± 2 years old with a diameter at breast height of 18.7 ± 2.1 cm and a height of 10.9 ± 1.4 m (see Table 1). The selected trees had grown on average 2.2 ± 1.2 mm y^{-1} in girth and 0.5 ± 0.1 m y^{-1} in height between 2012 and 2017.

2.2 | Experimental setup

One of four treatments—control, single compression, double compression or girdling—was randomly assigned to each tree, yielding 10 trees per treatment (Figure 1). The four treatment groups had similar age, initial diameter at breast height, height and average radial growth in the previous 5 years. Dead branches below 3 m were pruned in May 2017 to facilitate access to all stems.

The experiment started on the 4th of July 2017. For the control trees, no treatment was applied. For the girdling treatment, we carefully removed a 2.5 cm-wide strip of bark, phloem and cambium around the entire bole at 1.5 m stem height using razor blades (Figure 1). We did not seal or treat the wounds but subsequent callus growth was not sufficient to bridge the girdle in 2017. For the single compression treatment (hereafter "compression treatment"), collars were constructed from two ratcheted heavy-duty cargo belts with ratchets diametrically opposite each other as described in (Henriksson & Rademacher, 2019). Compression collars were removed after 36 days (10th August). For the double compression treatment, we installed identical sets of compression belts at 1.0 m and 2.0 m stem height (Figure 1) to isolate a stem section with regard to phloem transport to and from the canopy and the roots. Pressure underneath the belts was measured weekly using piezoelectric pressure sensors (Tactilus Free Form 12 mm, Sensor Products Inc., Madison, New Jersey, USA) to monitor exerted pressure over time. The belts generated a pressure exceeding 2 MPa around the entire circumference (Figure S1). We re-tightened the double compression belts after 38 days (13th August) to ensure that

TABLE 1 Summary statistics for the treatment groups including mean diameter at 1.5 m above the root collar, mean height ($\mu \pm 1\sigma$ for both), start and end date and duration

Treatment	*n*	dbh (cm)	*h* (m)	Start	End	Duration (days)
Control	10	18.2 ± 1.5	10.7 ± 1.6	–	–	–
Girdled	10	18.9 ± 2.2	11.1 ± 1.5	4th July	–	–
Compressed	10	18.2 ± 2.0	11.4 ± 0.7	4th July	10th August	36 days
Double compressed	10	19.7 ± 2.4	10.5 ± 1.7	5th July	10th October	95 days

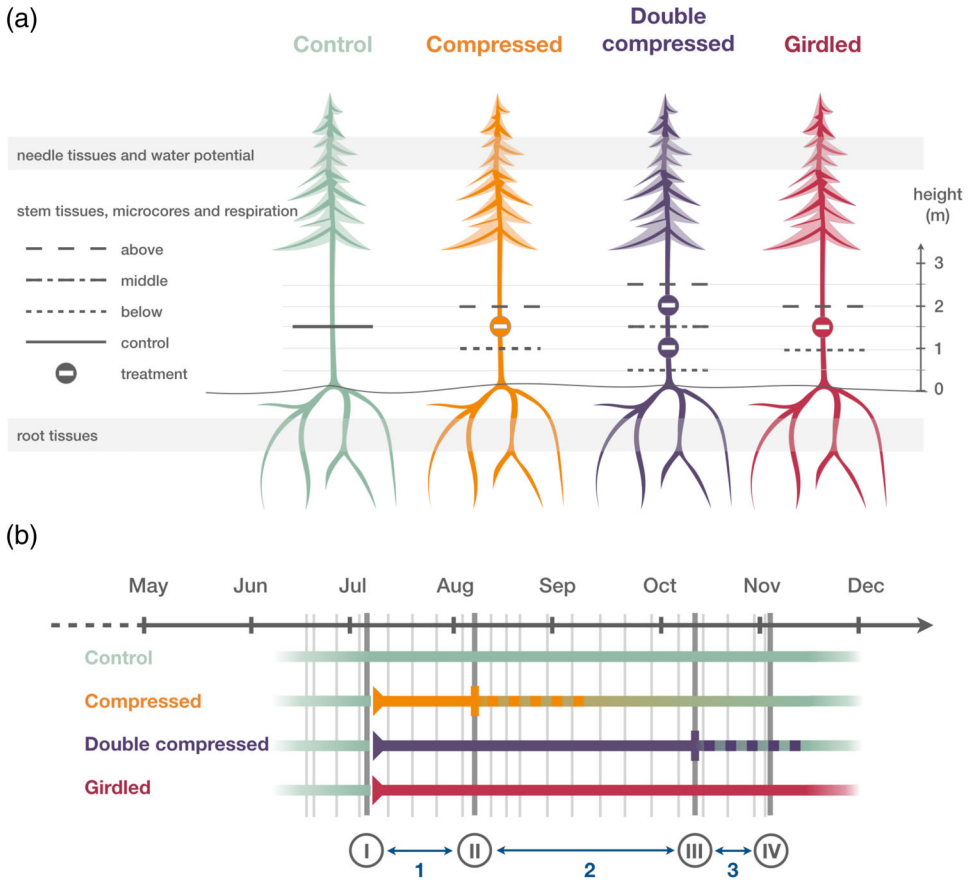

FIGURE 1 Experimental setup (panel a) and timeline (panel b). For all treated trees, stem measurements of CO_2 efflux, microcores and stem tissue samples were taken 0.5 m above (dashed lines) and below (dotted lines) the respective treatment. For double compressed trees, a third measurement in the middle of the two compression collars (dash-dotted line) was taken. For control trees, one measurement (solid line) was taken at 1.5 m. Additionally, root and needle tissue samples were collected. The experiment started in early July with baseline measurements directly followed by the experimental onset. Four dates of intensive sampling (I, II, III and IV) are indicated by thick, vertical, dark grey bars. On these sampling dates microcores and tissue samples for needles, stem wood and roots were collected. These dates divide the experiment into three distinct periods (1, 2, 3). Stem CO_2 efflux and water potential of needles and branches were measured weekly as indicated by the thinner, light grey, vertical bars

exerted pressures continually exceeded previous measurements of phloem internal pressure of 1 to 2 MPa (Nikinmaa, Sievänen, & Hölttä, 2014; Sovonick-Dunford, Lee, & Zimmermann, 1981; Wright & Fisher, 1980), despite potential loosening over time due to weathering (Figure S1a). We removed the belts of the double compression treatment after 95 days (10th October). We extended the duration of the double compression versus the single compression to investigate the effects of prolonged variations in carbon supply.

2.3 | Experimental monitoring

All trees were monitored during the experiment to characterize the carbon status of stem sections (Figure 1). Monitoring included a four-time characterization of tree-ring formation and nonstructural carbon concentrations in needle, stem and root tissues, and a weekly survey of stem CO_2 efflux until late November 2017. Two follow-up campaigns to measure CO_2 efflux were conducted in 2018, and an additional set of micrcores was collected in 2018.

Tree-ring growth was characterized from stem microcores collected at heights shown in Figure 1 with a Trephor (Rossi, Anfodillo, & Menardi, 2006) at five sampling dates. We collected microcores just before the treatments were imposed (3rd July), twice during the experiment (8th August and 10th October), and in late autumn of 2017 and 2018 (3rd November and 1st November, respectively). The microcores were stored in Eppendorf tubes containing a 3:1 solution of ethanol and glacial acetic acid. After 24 hrs, the solution was replaced with 95% ethanol. Micro-sections (7 μm-thick cross-sectional cuts) were cut with a rotary microtome (Leica RM2245, Switzerland) from paraffin-embedded samples (Tissue Processor 1020 Leica, Switzerland) and double-stained with astra-blue and safranin. Ring widths were measured using the Wood Image Analysis and Database platform (Rademacher, Seyednasrollah, Basler, et al., 2020) on microsection images captured using a digital slide-scanner (Zeiss Axio Scan. Z1, Germany) with a resolution of c. 1.5 pixels per μm. Tracheid anatomical characteristics (e.g., averages of cell size and cell-wall area over 20-μm wide tangential bands) were obtained using ROXAS 3.0.285 (von Arx & Carrer, 2014) from the November 2017 microsections (supplementary information S4).

Stem CO_2 efflux was measured weekly. Chambers (10 cm diameter by 10 cm length PVC pipe) were cut to fit each tree's stem curvature at all sampling heights (Figure 1) and attached 2 weeks prior to the treatments' start using silicone adhesive. Starting 1 week before the beginning of the treatments (29th June), an infrared gas analyzer (LI-820, LI-COR, Lincoln, Nebraska, USA) with a circulating pump (12K, Boxer, Ottobeuren, Germany) was attached to the chambers using a PVC cap with two ports to constantly circulate air through the closed system (Carbone et al., 2019). Once the concentration stabilized after closing the lid, the chamber CO_2 concentration was measured at 1 Hz for at least 1 min. Precautions were taken to minimize any effect of diel and environmental influences on treatment differences in CO_2 efflux (supplementary information S5). The raw stem CO_2 efflux and uncertainties were estimated using the RespChamberProc package (http://r-forge.r-project.org/projects/respchamberproc/) as developed by Perez-Priego et al. (2015).

Soluble sugar and starch concentrations in coarse roots, stems and needles were determined from tissue samples collected at the same time as the microcores (Figure 1). Coarse roots (at least 20 cm below the root collar) and stems were cored using an increment borer (5.15 mm diameter, Haglöf Company Group, Långsele, Sweden). Foliage samples were collected from a sun-exposed part of the crown with a pole pruner. All sampled tissues were immediately shock-frozen on dry ice in the field and subsequently stored in a freezer (−60°C) until being cut using razor blades and freeze-dried (FreeZone 2.5, Labconco, Kansas City, Missouri, USA and Hybrid Vacuum Pump, Vaccubrand, Wertheim, Germany). Dried samples were ground by Wiley mill with mesh 20 (Thomas Scientific Wiley Mill, Swedesboro, New Jersey, USA) and homogenized (SPEX SamplePrep 1600, MiniG, Metuchen, New Jersey, USA), although small samples were ground with an agate pestle and mortar (JoyFay International LLC, Cleveland, Ohio, USA) to minimize loss of material. An equal mix of first- and second-year needles (more than 100 needles from several branchlets) and the entire root core were each homogenized. For stems, we homogenized the first and second centimetre of xylem tissue separately. Bark and phloem were not included. Samples from July and November were analysed for the second centimetre to detect changes in deeper reserves. About 40 mg of finely ground and dried powder for all tissue, tree and sampling date combinations was analysed using a colourimetric assay with phenol-sulfuric acid following ethanol extraction according to the protocol by Chow and Landhausser (2004) as adopted by Furze et al. (2019). Colourimetric analysis was read twice at 490 nm for sugar and 525 nm for starch using a spectrophotometer (Thermo Fisher Scientific GENESYS 10S UV–Vis, Waltham, Massachusetts, USA), and calibrated with a 1:1:1 glucose:fructose:galactose (Sigma Chemicals, St. Louis, Missouri, USA) standard curve for sugar and glucose (Sigma Chemicals, St. Louis, Missouri, USA) standard curve for starch. Each batch of samples included on average 35 samples, at least 10 blanks—both tube and sample blanks—and between 9 and 12 laboratory control standards (red oak stem wood, Harvard Forest, Petersham, Massachusetts, USA; potato starch, Sigma Chemicals, St. Louis, Missouri, USA). We repeated extractions for batches that showed substantial deviations in the laboratory control standards (e.g., starch recovery fraction lower than 85%). The coefficient of variation for laboratory control standards was 0.08 and 0.09 for sugar and starch concentrations in oak wood, respectively, and 0.13 for potato starch. All samples' absorbance values were converted to concentrations in % dry weight and uncertainties with the self-developed R package NSCprocessR (https://github.com/TTRademacher/NSCprocessR).

To monitor tree water status, we measured pre-dawn needle and branch water potentials once per week per tree from the end of June to the beginning of November. Neither the two compression treatments, nor the girdling, affected tree water status (see Figure S2 for more details).

2.4 | Comparing carbon pools and fluxes in a stem section

We scaled mass growth, CO_2 efflux and net changes in soluble sugars and starch reserves in the first 2 cm of wood (hereafter stem sugar and starch reserves) to a common unit of grams of carbon in a stem section (height = 10 cm) for each experimental period (sensu Figure 1) to directly compare the sizes of these carbon fluxes. For structural carbon increments, we associated the cell-wall area for each 20-μm wide band with a date of formation using the fraction of the ring grown, which we derived from the microsections (i.e., from July, August, October). Cell-wall area was then divided by the width of the microcore and multiplied by the circumference and height of the stem section to get the cell-wall volume in the section. Finally, cell-wall volume was multiplied with a cell-wall carbon-density of 1.489 g cm^{-3} to estimate the mass of carbon fixed in the section (supplementary information S4). For losses due to CO_2 efflux, we averaged CO_2 efflux rates measured weekly for each period and multiplied them by the surface area of each stem section (supplementary information S5). To estimate nonstructural carbon reserves, we multiplied the average soluble sugar and starch concentrations in the first and second centimetre of the xylem, which are

assumed to be a large and the most easily accessible fraction of radial nonstructural carbon reserves (Furze et al., 2020; Richardson et al., 2015), with the volume of the hollow cylinder of that tissue. The net change in nonstructural carbon pools for a period was then computed as the difference between each pool's size at the end and the beginning of that period (supplementary information S6).

2.5 | Statistical analysis

We estimated treatment effects by fitting linear mixed-effects models with the lme4 package (Bates, Mächler, Bolker, & Walker, 2015) in R v3.6.3 (R Core Team, 2019). A tree identifier was included as a random effect to account for natural between-tree variability, and a fixed effect composed of an interaction between treatment and sampling height (e.g., above, middle and below) was added to substitute for the presumed carbon-supply gradient. When effects over time were estimated, we added date as a categorical fixed effect and to the treatment-sampling height interaction. Models were fitted using restricted maximum likelihood estimation. The strength and importance of estimated effects were judged in comparison with estimated variances. Hereafter, we report estimated effects ($\underline{\beta}$), their standard errors ($\underline{\sigma}$), and the t value in the following format: $\underline{\beta} \pm \underline{\sigma}$ ($t = t$). All code and data are publicly available on the Harvard Forest Data Archive (Rademacher & Richardson, 2020).

3 | RESULTS

3.1 | Effects on carbon allocation

The treatments had clear effects on growth and CO_2 efflux, but not on nonstructural carbon pools (Figure 2). The mass of new wood growth mirrored the presumed carbon-supply gradient. Above the compression, double compression and girdle an additional 20%, 139% and 92% (respectively) of carbon was sequestered in newly formed wood relative to the control from July to November (Figure 2). Below both compression and double compression, mass growth was not discernibly different from the control from July to November. However, wood formation ceased completely below the girdle roughly 1 month after the girdling, approximately halving carbon sequestration in the woody structure during the experimental period. CO_2 efflux was higher above all treatments (46% above compression, 124% above double compression and 111% above the girdle) between July and November relative to the control. Stem CO_2 efflux was also substantially reduced below treatments (−45% for compression, −42% for double compression and −70% for girdling) relative to the control, even when mass growth and the number of forming cells was not noticeably impacted below the compression treatments (Figures 2 and 3). Over the same period, net changes in nonstructural carbon reserves in the stems were more than an order of magnitude smaller than the estimated carbon allocation to growth and stem CO_2 efflux (Figure 2). A detectable treatment effect on nonstructural carbon concentrations was only apparent in girdled trees.

3.2 | Resulting wood characteristics

About 60% of the final ring width had already formed in control trees by the experimental onset (4th July). Control trees showed a typical progression toward smaller tracheids with thicker cell walls over the remainder of the growing season (Figure 3), resulting in an average of 51 cells per radial file composing a 1.28 mm-wide ring for 2017.

Above the treatments, radial growth was stimulated in the double compression and girdled trees. The final ring above the double compression and girdle was on average 0.73 ± 0.18 mm ($t = 5.24$) or 57%,

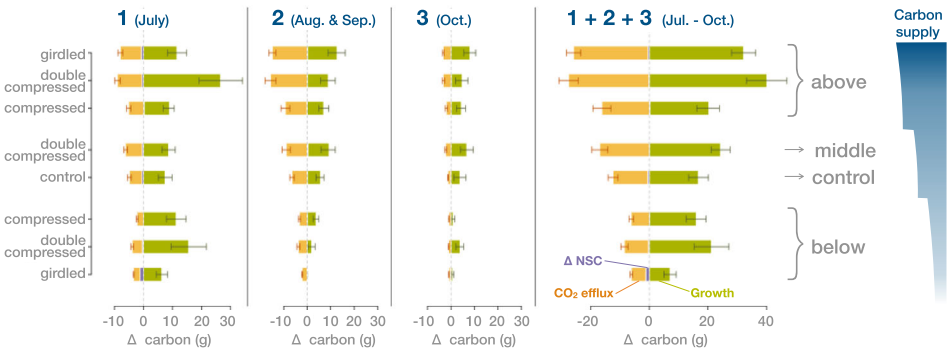

FIGURE 2 Carbon budget (integral of mass growth, losses due to CO_2 efflux and net change in nonstructural carbon pools in the first centimetre) for an average 10 cm-high stem section over three periods. Sections are sorted along a presumed carbon-supply gradient from highest above the girdle to lowest below the girdle illustrated schematically on the right. The panel numbers correspond to the periods indicated in the timeline (Figure 1): (1) first month of the experiment (e.g., mostly July), (2) second and third month after experimental onset (e.g., mostly August and September) and (3) fourth month after experimental onset (e.g., mostly October). The panel (1 + 2 + 3) shows the cumulative changes from the beginning of July to November. Losses due to CO_2 efflux (orange), radial mass growth (green), and net changes in total nonstructural carbon pools in the first centimetre (purple) are shown for each treatment and sampling height (A = above, B = below, M = middle and C = control). Error bars indicate one standard error. For details on the scaling assumptions of structural carbon, CO_2 efflux, and nonstructural carbon see supplementary information S4–S6, respectively [Colour figure can be viewed at wileyonlinelibrary.com]

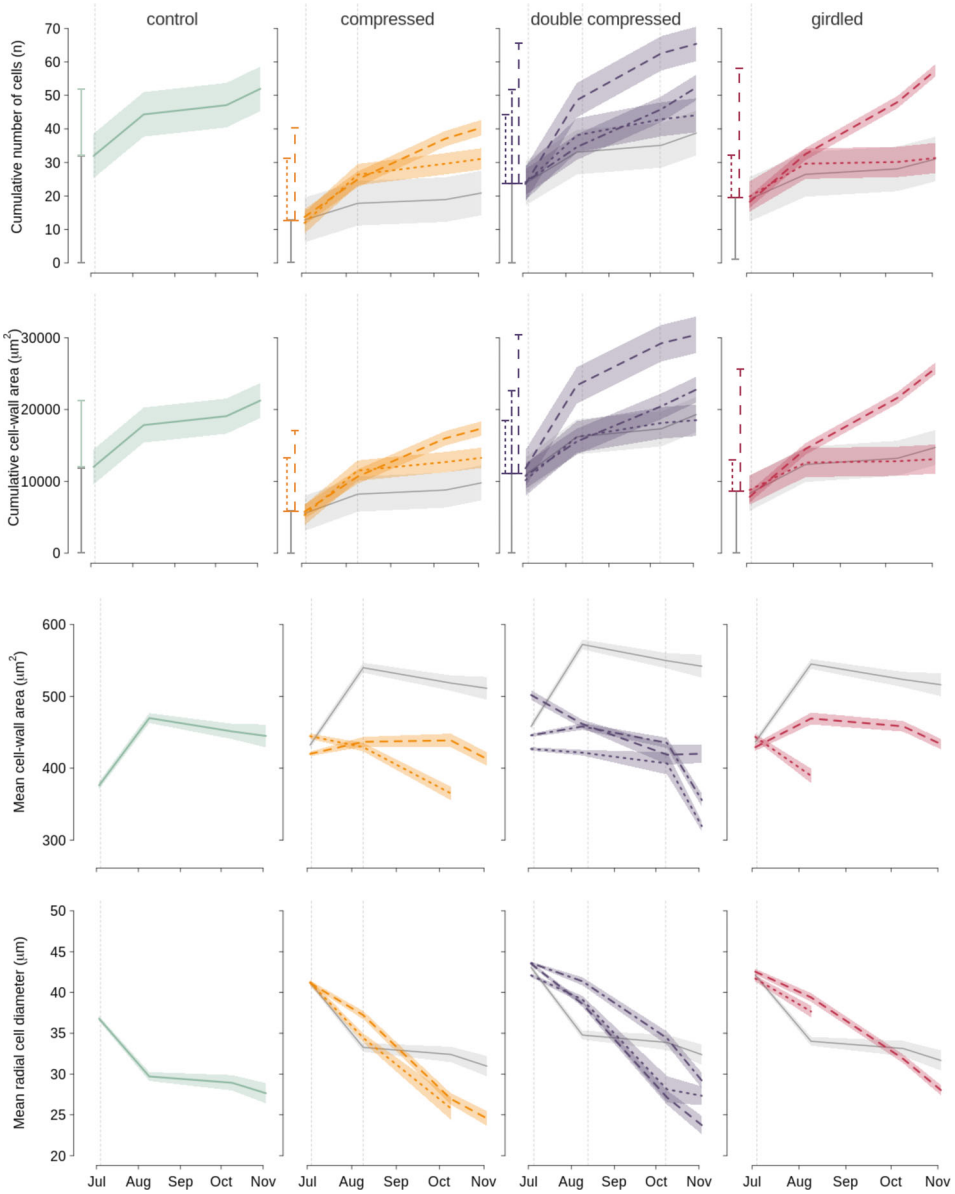

FIGURE 3 Treatment effects on the wood formation and the resulting anatomy in stem sections of control trees (solid line), as well as above (dashed lines), in the middle of (dash-dotted line) and below (dotted line) treatment zones of treated trees over time. For stem sections from control (left column; green), compressed (second column; orange), double-compressed (third column; purple) and girdled trees (right column; red), we show the cumulative number of cells (top row), the cumulative cell-wall area (second row), mean cell-wall area per cell (third row) and mean radial cell diameter (fourth row). For the cumulative number of cells and cell-wall area, total contributions prior (grey) and after (colour) the experimental onset are summarized on the left of each graph. Lines and shading indicate the mean and one standard error and are coloured by treatment. Means are not displayed when the average period growth did not exceed 0.05 mm (n < 25 20-µm wide zones). For ease of comparison, the control group is normalized to each treatment's July baseline and displayed in grey. Dashed grey vertical lines indicate key dates for each treatment, such as start date, re-tightening date and end date [Colour figure can be viewed at wileyonlinelibrary.com]

and 0.57 ± 0.18 mm ($t = 4.33$) or 45% wider than the control. However, the ring width was not clearly wider above the compression relative to the control with an additional 0.15 ± 0.18 mm ($t = 1.90$) or 12%. Differences in ring width could mainly be traced to changes in the number of cells formed after treatment onset, rather than their sizes. All three treatments formed unequivocally fewer cells below the treatment versus above with a difference of 10 ± 6 ($t = 1.67$) or 33% for compressed, 21 ± 4 ($t = 5.25$) or 51% for double compressed and 27 ± 3 ($t = 9.00$) or 93% for girdled trees. Control and treated trees had similar radial cell diameters (Figure 3). Mean cell-wall area declined slightly below treatments but did not differ above the treatments relative to the control (Figure 3). Combined with large differences in the number of cells per radial file above and below treatments, the relatively smaller differences in average cell-wall area caused substantial differences in cumulative cell-wall area, and hence structural biomass.

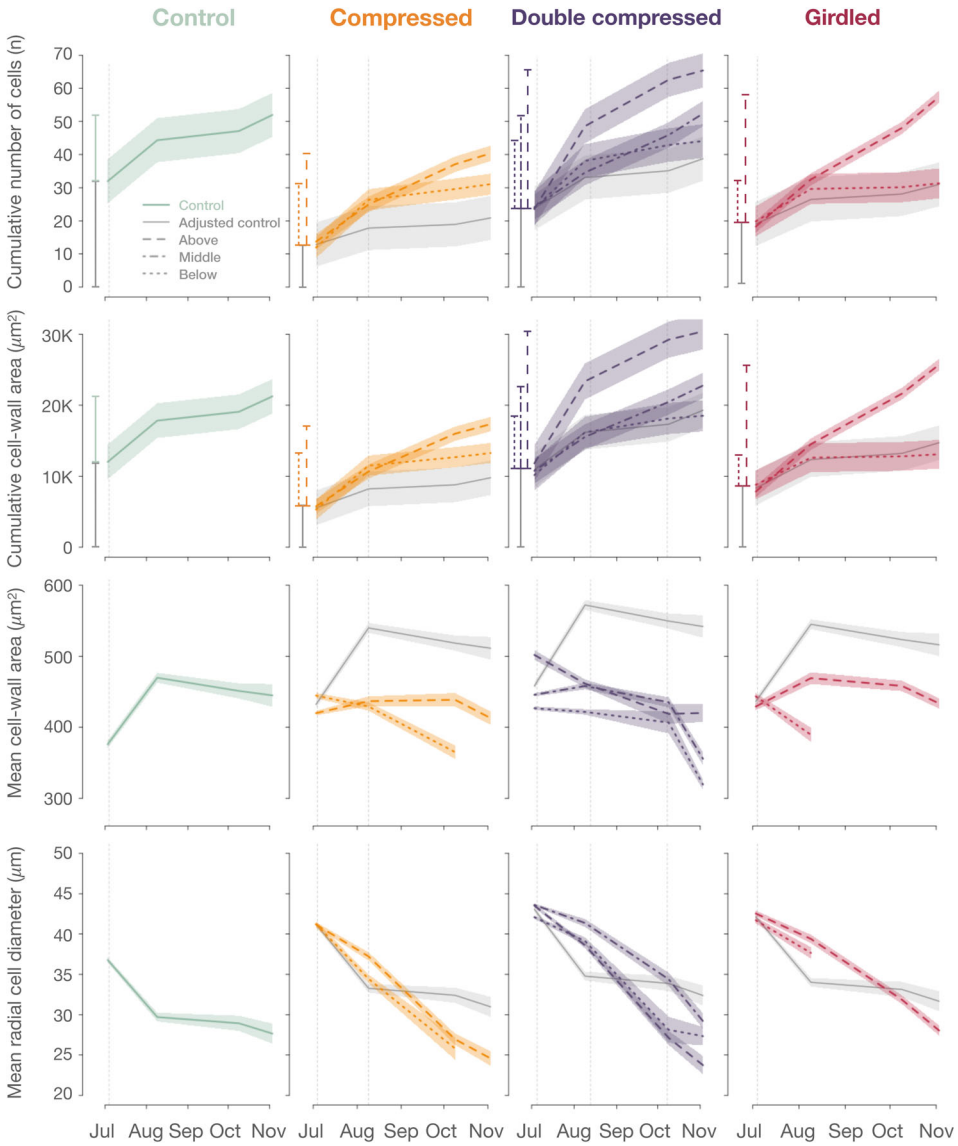

FIGURE 3 (Continued)

Below the girdle marginally narrower rings (−220 ± 176 [$t = -0.18$] μm or −17%) with slightly lower mean cell-wall area formed compared to the control (Figure 3). Mean cell-wall area was reduced by 75 ± 29 ($t = -2.55$) μm^2 or 18% below the girdle by August relative to the control. Below the compression, the reduction relative to the control was 47 ± 32 ($t = -1.49$) μm^2 or 12% by October. After August and October, too few cells formed below the girdle and compression, respectively, to reliably quantify these trends further. In the middle and below the double compression enough cells formed to detect a pronounced decline in mean cell-wall area of −134 ± 32 ($t = -4.21$) μm^2 or −35% and −64 ± 31 ($t = -2.06$) μm^2 or −17%, respectively, by November.

Above the girdle, growth resumed in 2018 for 9 of the 10 trees at an average of 120 ± 43% of the standardized ring width of the control group (data not shown). However, only two trees showed any sign of growth below the girdle in 2018 at 9 and 81% of standardized ring width. 19 out of 20 compressed trees grew radially in 2018 (e.g., more than 6 months after the compression belt removal) at 78 ± 15% and 69 ± 16% of the control group growth above and below the compression and 107 ± 11%, 60 ± 11% and 56 ± 20% of the control group above, in the middle and below the double compression, respectively.

3.3 | Effects on stem CO_2 efflux

Stem CO_2 efflux of the control group generally declined after a maximum at the start of the experiment (Figure 4). Losses of carbon due to CO_2 efflux generally mirrored mass growth in pattern and magnitude across the gradient of carbon supply, but losses due to CO_2 efflux were more markedly reduced than growth below both compression treatments (Figure 2). Treatment effects on CO_2 efflux lagged 2–3 weeks behind the treatment onset (Figure 4). Over the remaining

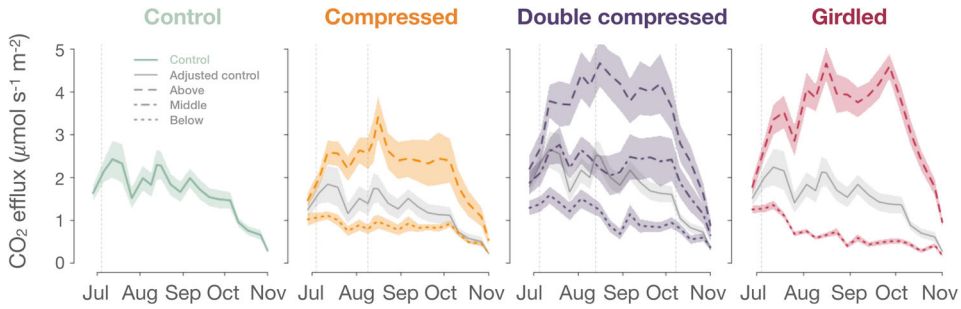

FIGURE 4 Mean stem CO_2 efflux (line) and one standard error (shading) by treatment (colour) and sampling height (line type) over time. For reference, the control group mean and standard error are normalized to the treatment baselines and plotted in grey in the background for all other treatments. The grey vertical dashed lines mark the appropriate key dates for each treatment, such as start date, re-tightening date and end date [Colour figure can be viewed at wileyonlinelibrary.com]

growing season after the treatment onset, the average stimulation of stem CO_2 efflux above the treatment amounted to 56 ± 14% ($t = 2.39$), 150 ± 15% ($t = 6.19$) and 132 ± 14% ($t = 5.64$) of the control for compression, double compression and girdling, respectively. Below the compression, double compression and girdle, CO_2 efflux fell by on average 48 ± 14% ($t = -3.43$), 38 ± 14% ($t = -2.52$) and 82 ± 14% ($t = -3.17$) of the control for the period of the treatment. Between the double compression collars, CO_2 efflux stayed close to the control with an increase of 28 ± 21% ($t = 1.86$) during the compression. By November, both compression treatments' CO_2 efflux rates had converged and remained indistinguishable from the control treatment for the following growing seasons (data not shown).

3.4 | Changes in nonstructural carbon

Nonstructural carbon concentrations, in particular soluble sugars, varied little among treatments and sampling heights. Needle, wood and root tissues averaged soluble sugar concentrations of 8.33 ± 0.17%, 0.83 ± 0.01% and 1.47 ± 0.05%, with starch concentrations of 1.32 ± 0.14%, 0.28 ± 0.01% and 0.31 ± 0.03% across all four measurement dates and trees, respectively. In tissues above all treatments, soluble sugar concentrations mostly followed the typical seasonal fluctuation of the control group but increased slightly in a few tissues (Figure 5). Most notably, increases in needle soluble sugar concentrations were observed in girdled trees, peaking at an additional 3.30 ± 1.28% ($t = 2.58$) in November. Needle starch concentrations in girdled trees were also higher in August and October but had mostly converged (0.44 ± 0.88% [$t = 0.49$]) with the control by November (Figure 6). Higher needle soluble sugar concentrations were also apparent for compressed and double compressed trees, albeit with substantially smaller increases than for the girdled trees, culminating in November at 0.56 ± 1.26% ($t = 0.44$) and 2.38 ± 1.26% ($t = 1.88$), respectively. Finally, wood sugar concentrations above the treatments increased marginally in the first centimetre by 0.42 ± 0.16% ($t = 2.64$), 0.35 ± 0.15% ($t = 2.22$) and 0.23 ± 0.16% ($t = 1.44$) for compression, double compression and girdling by November, whereas wood starch concentrations remained stable above all treatments but declined below the girdle by 0.32 ± 0.07% ($t = -4.48$) relative to the control in November. Changes in nonstructural carbon concentrations in the second centimetre of the wood by November were similar to the changes in the first centimetre, but smaller (Figure S3). Furthermore, the observed treatment effects on wood nonstructural carbon concentrations were comparatively small in relation to the seasonal variation (Figure 6). With the exception of a decrease in root starch of 0.65 ± 0.17% ($t = -3.83$) relative to the control, nonstructural carbon concentrations were similar in tissues below the treatments.

4 | DISCUSSION

Growth and CO_2 efflux covaried with the presumed carbon-supply rate, but the sizes of nonstructural carbon pools did not change substantially. Thus, we have to partially reject our first hypothesis (H1) of constant ratios of carbon allocated to newly formed structural carbon, local bulk nonstructural carbon reserves and CO_2 efflux across the presumed gradient of carbon supply. In contrast to our hypothesis, the proportion of carbon allocated to local storage varied substantially. Under lowered carbon supply, a larger proportion of carbon was allocated to nonstructural carbon pools, maintaining seasonal values similar to the control group. A similar prioritization of nonstructural carbon reserves overgrowth has been observed elsewhere under lowered carbon supply at the whole-tree level in response to defoliation (Piper, Gundale, & Fajardo, 2015; Wiley, Casper, & Helliker, 2017), drought (Hagedorn, Joseph, Peter, et al., 2016) and reduced atmospheric CO_2 (Hartmann, McDowell, & Trumbore, 2015; Huang et al., 2019). Under elevated carbon supply, the amount of carbon allocated to respiration and formation of woody tissues was higher compared to the control in our study. This contrasts with whole-tree effects of proportionally larger increases in nonstructural carbon concentrations than stimulations of wood growth under elevated CO_2 (Ainsworth & Long, 2005; Körner et al., 2005), whereas previous direct phloem manipulations support our observed shift in allocation towards growth at elevated carbon supply above the treatment (De Schepper et al., 2011; Maier et al., 2010; Oberhuber, Gruber, Lethaus, Winkler, & Wieser, 2017; Regier et al., 2010). The

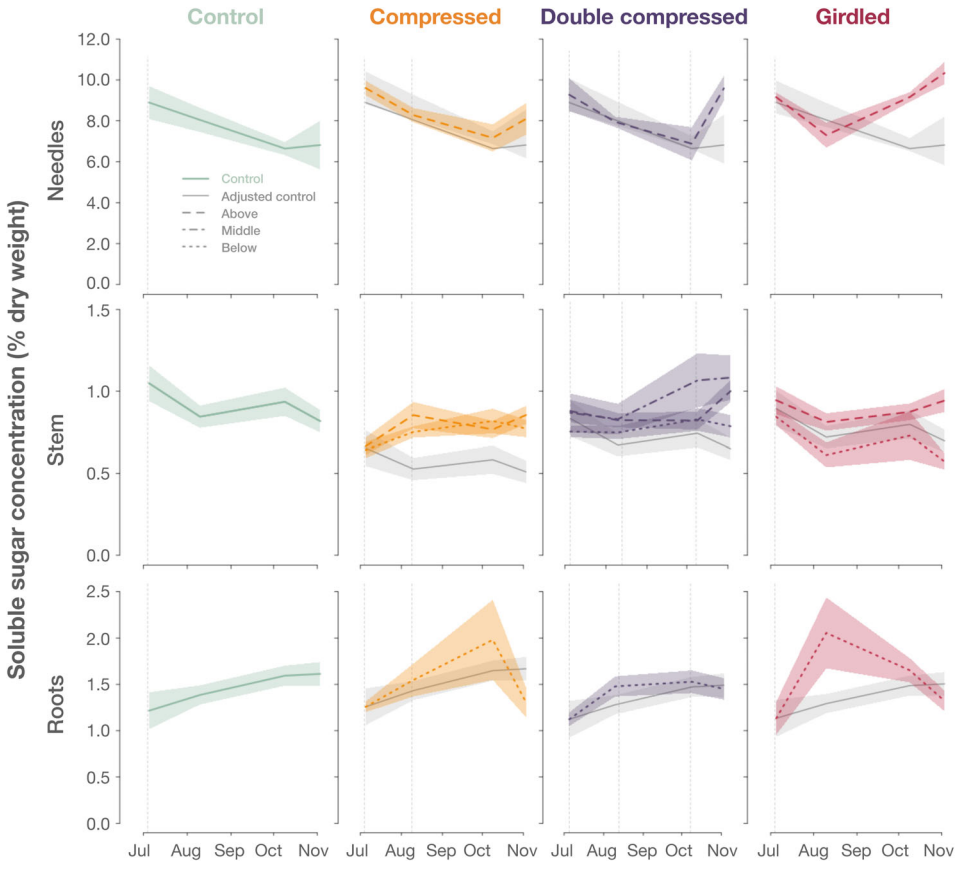

FIGURE 5 Soluble sugar concentrations in needles (top row), the first centimetre of the xylem (middle row) and coarse roots (bottom row) for the control (left column; green), compressed (second column; orange), double-compressed (third column; purple) and girdled (right column; red) trees over time. Coloured lines and shading show the mean and one standard error with colours corresponding to the treatment. Line type corresponds to the spatial positioning relative to the treatment with solid lines for control, dashed lines for above the treatment, dotted lines for below and dash-dotted lines for in the middle of two treatment zones. For ease of comparison, the control group is adjusted for baseline differences and added to all treatment panels (grey line and shading). Key dates—start, retightening of compression collars and end date—are indicated by grey, dashed vertical lines [Colour figure can be viewed at wileyonlinelibrary.com]

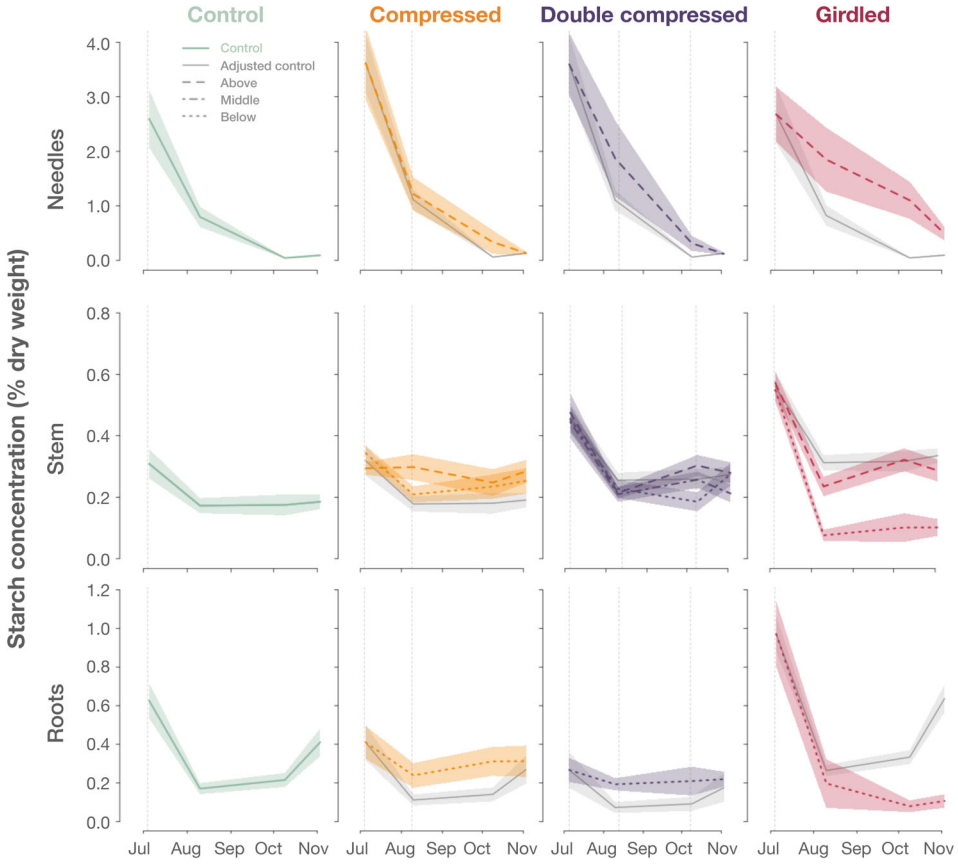

FIGURE 6 Starch concentrations in needles (top row), the first centimetre of the xylem (middle row), and coarse roots (bottom row) for the control (left column; green), girdled (second column; orange), compressed (third column; purple) and double compressed (right column; red) trees over time. Coloured lines and shading show the mean and one standard error with colours corresponding to the treatment. Line type corresponds to the spatial positioning relative to the treatment with solid lines for control, dashed lines for above the treatment, dotted lines for below and dash-dotted lines for in the middle of two treatment zones. For ease of comparison, the control group is adjusted for baseline differences and added to all treatment panels (grey line and shading). Key dates—start and end date as well as date of re-tightening—are indicated by grey, dashed vertical lines [Colour figure can be viewed at wileyonlinelibrary.com]

apparent discrepancy between results of whole-tree and phloem transport manipulations of carbon supply may result from differences in signalling, size and/or species, but we cannot rule out either within-tree feedbacks at elevated CO_2, such as non-stomatal downregulation of photosynthesis (Salmon et al., 2020) or redistribution of carbon throughout the entire tree. In line with the redistribution of carbon throughout the tree, we saw the largest changes in non-structural carbon reserves in foliage and roots. Overall, we found that carbon use by wood growth and CO_2 efflux is much more sensitive to variations in carbon supply than are local bulk nonstructural carbon pools, resulting in rejection of H1.

4.1 | Wood growth was correlated with carbon supply

Our second hypothesis (H2), that differences in growth between treatments and sampling heights are driven by differences in cell numbers was supported. However, despite a small reduction of mean cell-wall area below the treatments, we have to reject our third hypothesis (H3) that differences in mean cell-wall area are another important driver of differences in structural biomass with carbon supply, as differences in cumulative cell-wall area among treatments could be mainly attributed to differences in cell numbers. For example, we did not see an increase in mean cell-wall area at higher presumed carbon supply above treatments. We found evidence supporting our fourth hypothesis (H4), that cell size does not vary with carbon supply.

Availability of soluble sugars is linked to cell division in plants through metabolic signalling (Lastdrager et al., 2014; Riou-Khamlichi et al., 2000; Smith & Stitt, 2007), which could explain the observed pattern in cell numbers. Soluble sugar concentrations also influence the osmotic potential in cambial cell lumens which affects turgor pressure (Guerriero, Sergeant, & Hausman, 2014), hence growth (Cabon et al., 2020; Peters et al., 2021. Previously, modelling (De Schepper & Steppe, 2011) and experimental evidence from saplings (Winkler & Oberhuber, 2017) were interpreted to suggest that an accumulation of osmotically active sugars in the cambium was responsible for observed increases in cell division due to consequent changes in turgor pressure. We did not see a difference in soluble sugar concentrations in the first or second centimetre of the xylem between control and treated trees and among sampling heights, despite large differences in the number of cells formed. Previous studies found strong radial gradients in soluble sugar concentrations in the cambial region (Uggla, Magel, Moritz, & Sundberg, 2001), which together with our comparatively coarse measurement resolution (e.g., 1 cm of xylem not including the cambium) does not preclude that a turgor-mediated mechanism caused the observed increase in cell numbers. Interestingly, cell size was not affected here, suggesting that any osmotic (or water status) effect on turgor pressure and subsequently on cell enlargement rate was presumably compensated for by an opposite effect on enlargement duration, as increases in cell division would accelerate the progression of the development. While limitation in carbon supply due to natural defoliation can reduce growth (Fierravanti, Rossi, Kneeshaw, De Grandpré, & Deslauriers, 2019) and cell numbers substantially (Castagneri et al., 2020), we found that the cumulative number of cells formed, thus cell division seems to be regulated by carbon supply more generally (including at elevated carbon supply).

Contrary to a previous study on saplings (Winkler & Oberhuber, 2017), we did not see a reduction in cell-wall area per cell above the girdle or the compression treatments. This reduction in cell-wall deposition per cell at higher carbon supply was attributed to either additional carbon demand due to more cells formed or alternative investment in defense compounds due to a wound reaction. Winkler & Oberhuber et al. (2017) also reported the formation of smaller lumen diameters in earlywood above the girdle and larger lumen diameters in latewood, in contrast to our findings of no substantial changes in cell size and wall area. We cannot rule out that differences in phenology, especially because earlywood formation was advanced at the onset of our experiment, or species may be responsible for the differing effects on cell-wall deposition and cell size. Nonetheless, we suspect that the differences are caused by different ontogenetic stages: saplings versus mature trees, as trees are thought to be more carbon limited at younger ages (Hartmann et al., 2018; Hayat et al., 2017; Körner, 2003). Strong ontogenetic effects on the relationship between carbon supply and wood formation call into question whether knowledge on source-sink relationships generated using seedlings or saplings is directly transferable to mature trees. Together, changes in cell production and cell-wall deposition led to a marked increase in cumulative cell-wall area, and thus biomass, suggesting that increased carbon supply leads to proportional increases in volume and mass growth (mainly due to increases in cell number with constant cell characteristics).

Our finding of no difference in cell size with presumed variations in carbon supply support that intra-annual transitions in cell size are mainly constrained developmentally due to compensatory effects of rate and duration of cell elongation (Balducci et al., 2016; Cuny & Rathgeber, 2016). Dynamic soluble sugar concentrations in the cambium have been argued to drive this early-to-latewood transition by determining the rate of cell-wall deposition with a threshold cell-wall thickness regulating the end of cell elongation, hence cell size and mean cell-wall area (Cartenì et al., 2018). Our observed, albeit small decline in mean cell-wall area at low carbon supply is in line with the proposed mechanism. However, the observed insensitivity of cell size contrasts with the mechanisms put forward by Cartenì et al. (2018), which would presumably result in smaller cells at higher carbon supply. Rates of cell elongation gradually decline over the growing season (Cuny et al., 2018), therefore they are likely to be more sensitive in the early growing season. While cell size was insensitive to carbon supply here, an earlier start date might still reveal a relationship between cell elongation, hence their size, and carbon supply.

Primarily varying the number of cells formed in response to carbon supply to wood forming tissues with cell morphologies largely unchanged may have evolved in conifers to reduce risks of disrupting water transport and mechanical support, which are intricately linked to the cells' anatomical characteristics, such as lumen diameter for water transport (Sperry, 2003; Tyree & Zimmermann, 2002) and lumen to cell-wall area ratio for mechanical support (Niklas, 1992).

4.2 | CO_2 efflux covaried with carbon supply

Stem CO_2 efflux covaried with the presumed carbon supply and total fluxes were slightly smaller than carbon sequestration due to growth over the treatment period. CO_2 efflux rates responded within about 1 week to phloem transport manipulations but took several weeks to relax to control group values once the compression was removed. The only other stem-compression study we are aware of documented a similar effect on stem CO_2 efflux, but a faster recovery of only 2 weeks for mature Scots pines (Henriksson et al., 2015). We suspect that this discrepancy in recovery rate is caused by our experiment ending later in the growing season when phloem growth and hence presumably recovery is less vigorous. The compression collar design used here also exerted slightly higher pressure around the circumference (Henriksson & Rademacher, 2019), which may have contributed to the longer observed recovery times and continued effects in double compressed trees on radial growth in the following growing season.

Stem CO_2 efflux declined as much below compression treatments as below girdles, despite mass growth remaining at control group levels below both compression treatments. CO_2 efflux therefore appears more sensitive than mass growth to reduced carbon supply. The continuation of growth below the compression treatments could mean that non-growth metabolism is preferentially downregulated at lower carbon supply. CO_2 efflux and growth may preferentially draw on different carbon sources (i.e., phloem-transported, which may have leaked across the compression only, vs. local stores). Indeed, isotopic studies have revealed that respiration preferentially uses younger carbon from recent assimilates, while growth can draw on reserves of carbon when recent assimilates are scarce (Maunoury-Danger et al., 2010). Similar CO_2 efflux levels below the girdle and both compression treatments may suggest that they both approached a necessary minimum that is essential to maintain living tissue (Minchin & Lacointe, 2005). Because wood formation commits more than the instantaneously required resources, it could be argued that respiration is preferentially down-regulated to maintain reserves needed to fuel and provide resources for cells that have just divided, but will still require energy and resources to elongate, thicken their cell walls and lignify. Given the lack of an equivalent local depletion of nonstructural carbon reserves below treatments, it is possible that the majority of the carbon necessary to fuel CO_2 efflux was supplied from root reserves in the girdled trees, which declined more substantially, and from leakage across the compression zone in compressed trees.

4.3 | Wood soluble sugar and starch concentrations were stable across a large carbon-supply gradient

With regard to nonstructural carbon reserves, soluble sugar concentrations remained remarkably constant for any individual compartment among treatments and tissues. One exception was increased in needle soluble sugar concentrations in girdled trees towards the end of the growing season, which may cause non-stomatal photosynthetic down-regulation (Salmon et al., 2020) and more generally trigger whole-plant feedbacks. In contrast to stable sugar concentrations, starch concentrations varied in a few tissues, potentially compensating for imbalances in carbon supply and demand to stabilize soluble sugar concentrations homeostatically. Noticeable remobilization and accumulation of starch were most apparent in the roots and needles of girdled trees, respectively, and to a lesser degree in the double compression. Overall, the net changes of nonstructural carbon reserves were, however, marginal compared to investments in growth and losses to CO_2 efflux.

The observed stable soluble sugar concentrations across treatments add to previous evidence that nonstructural carbon concentrations follow relatively constrained seasonal cycles in the wood of mature trees (Zhang et al., 2020). Soluble sugar concentrations seem to be generally maintained to follow a specific seasonal rhythm. Consequently, equating high wood soluble sugar concentrations with a sink limitation (Hagedorn et al., 2016) may not be a reliable interpretation, because growth and wood soluble sugar concentration seem to be regulated independently under varying carbon supply here and in previous studies (Weber, Gessler, & Hoch, 2019). Given the steep concentration gradients across developing wood (Uggla et al., 2001) and the importance of sugar concentrations, as a potential regulator for various developmental phases (De Schepper & Steppe, 2011; Cartenì et al., 2018), further phloem transport manipulations measuring sugar concentrations at a higher spatial resolution using microdissection would help to better understand the role of cambial sugar concentrations on wood formation.

4.4 | Phloem compression as a reversible alternative to girdling

Our observations suggest that phloem compression was successful as an alternative to girdling to manipulate phloem flow. Similar to Henriksson et al. (2015), we observed diverging CO_2 efflux rates above and below compression treatments during the compression period and convergence thereafter. The growth increase, especially above the double compression treatment, further suggests that the treatment generated an effective bottleneck for phloem transport, leading to enhanced carbon and/or hormone supply above the treatment. However, the small increase above the single compression and similar growth below the compression treatments relative to the control, without substantial depletion of connected nonstructural carbon reserves, suggests that phloem flow was only reduced and not halted completely. Wood also continued to form between the double compression collars with CO_2 efflux rates roughly equaling control group rates without substantially reducing the local xylem nonstructural carbon reserves, indicating that some carbon continued to be transported across the compression zones. Because phloem compression was effective, albeit somewhat leaky, phloem transport seems to have been successfully modified to generate our hypothesized carbon-supply gradient ranging from severe carbon limitation below the girdle, over moderate carbon limitation below the compression (due to

some leakage) and moderate carbon supply surplus above the compression, to a larger surplus above the girdle. The simultaneous reduction in other phloem-transported signaling compounds, which are essential for wood formation (Aloni, 2013; Buttò et al., 2020), may have influenced our observed results given that phloem transport is a mass flow.

Multiple studies using girdling have shown that stopping phloem transport causes an early cessation of cambial activity (Maunoury-Danger et al., 2010; Oberhuber et al., 2017). Our results showed that new cells formed below both compression treatments after removal in the same (20 out 20 trees) and the following (19 out 20 trees) growing season, indicating that the phloem can recover from compression and carbon and/or hormone availability can re-activate the cambial meristem once the phloem has recovered. A similar number of cells formed below the single compression relative to control after the date of removal of the compression, but slightly fewer cells formed below the double compression (possibly due to later release). Mass growth after the date of removal of the compression was similar to the control group, suggesting that growth resumed at normal levels and there was no compensatory enhancement of growth. While our sampling frequency did not allow for the precise identification of critical dates of wood formation, our results show that cambial activity is dependent on intact phloem transport and that compressed phloem tissue can partially recover late into the growing season (here early October). Nevertheless, the compression had lagged effects on wood formation in compressed trees in the following season, suggesting that full recovery takes more than one growing season. Temporal plasticity of radial growth has recently been reported as a response to environmental constraints (Zhang et al., 2020). Yet, the temporal and spatial plasticity of growth exhibited through local variations in wood formation in our study among treatments and sampling heights suggests that the mechanism controlling this plasticity operates directly in the cambial region and can be triggered without environmental clues. Spatial variations in radial growth of the same tree, which are typically considered to be noise by dendrochronologists, may hold clues about local differences in carbon supply. Overall, phloem compression appears to be an exciting tool to help understand which physiological processes may be carbon-supply limited, over which timescales, and during what time of the year.

4.5 | Conclusion

Restricting phloem transport by compressing and girdling trees has illustrated homeostatic maintenance of local xylem bulk nonstructural carbon reserves along a presumed large gradient of carbon supply, whereas wood growth and CO_2 efflux covaried with carbon supply. Consequently, local bulk nonstructural carbon is clearly not a simple reserve to fuel growth and respiration but seems to be regulated independently. Concerning wood formation, cell division seems particularly sensitive to carbon supply with minor additional effects on cell-wall deposition. Overall, wood formation seems to be carbon-limited locally.

ACKNOWLEDGMENTS

A.F., A.R., T.R., and Y.C. acknowledge support from the Natural Environment Research Council (NE/P011462/1) and National Science Foundation (DEB-1741585). A.R. is also supported by the National Science Foundation under grants DEB-1237491 and DEB-1832210. D.B. acknowledges support through the Swiss National Science Foundation (PSBSP3-168701) and the Harvard Forest Bullard Fellowship. We also thank Aglaé Landry-Boisvert, Brooklynn Abaroa, Emory Ellis, Kyle Wyche and Mark VanScoy for help in the field, Shawna Greyeyes, Amberlee Pavey and Angelina Valenzuela for help in the lab, Katharyn Duffy, Teemu Hölttä, Drew M. P. Peltier and three anonymous reviewers for feedback on the manuscript and Henrik Hartmann, Nils Henriksson, Teemu Hölttä and Cyrille Rathgeber for friendly peer-review of the ideas and methods.

CONFLICT OF INTEREST

The authors declare no conflict of interest.

AUTHOR CONTRIBUTIONS

Tim Rademacher and Andrew D. Richardson planned and designed the experiment. Tim Rademacher conducted the experiment, collected all data and materials. Tim Rademacher, James M. LeMoine, Marina V. Fonti, and Patrick Fonti conducted the laboratory analyses. Bijan Seyednasrollah, David Basler and Tim Rademacher created the TRIAD platform. Tim Rademacher developed the NSCprocessR package with input from James M. LeMoine and Andrew D. Richardson. Tim Rademacher performed the statistical analysis, generated the figures, and wrote the paper. All co-authors discussed ideas, provided feedback, edited the manuscript draft and approved the manuscript for submission.

DATA AVAILABILITY STATEMENT

All data and code to reproduce the results and figures are publicly available on the Harvard Forest Data Archive as data set HF348 (Rademacher & Richardson, 2020).

ORCID

Tim Rademacher https://orcid.org/0000-0002-0627-6564
Patrick Fonti https://orcid.org/0000-0002-7070-3292
Marina V. Fonti https://orcid.org/0000-0002-2415-8019
David Basler https://orcid.org/0000-0002-4068-8319
Yizhao Chen https://orcid.org/0000-0002-9218-6679
Andrew D. Friend https://orcid.org/0000-0002-9029-1045
Bijan Seyednasrollah https://orcid.org/0000-0002-5195-2074
Annemarie H. Eckes-Shephard https://orcid.org/0000-0002-2453-3843
Andrew D. Richardson https://orcid.org/0000-0002-0148-6714

REFERENCES

Ainsworth, E. A., & Long, S. P. (2005). What have we learned from 15 years of free-air CO_2 enrichment (FACE)? A meta-analytic review of the responses of photosynthesis, canopy properties and plant production to rising CO_2. *New Phytologist*, *165*, 351–372.

Aloni, R. (2013). Role of hormones in controlling vascular differentiation and the mechanism of lateral root initiation. *Planta*, *238*, 819–830.

Atkin, O. (2015). New Phytologist and the 'fate' of carbon in terrestrial ecosystems. *New Phytologist*, *205*, 1–3.

Balducci, L., Cuny, H., Rathgeber, C., Deslauriers, A., Giovannelli, A., & Rossi, S. (2016). Compensatory mechanisms mitigate the effect of warming and drought on wood formation: Wood formation under warming and drought. *Plant, Cell & Environment*, *39*(6), 1338–1352.

Bates, D., Mächler, M., Bolker, B., & Walker, S. (2015). Fitting linear mixed-effects models using lme4. *Journal of Statistical Software*, *67*, 1–48.

Begum, S., Kudo, K., Rahman, M. H., Nakaba, S., Yamagishi, Y., Nabeshima, E., … Funada, R. (2018). Climate change and the regulation of wood formation in trees by temperature. *Trees*, *32*(1), 3–15. http://dx.doi.org/10.1007/s00468-017-1587-6.

Björklund, J., Seftigen, K., Schweingruber, F., Fonti, P., von Arx, G., Bryukhanova, M. V., … Frank, D. C. (2017). Cell size and wall dimensions drive distinct variability of earlywood and latewood density in northern hemisphere conifers. *New Phytologist*, *216*, 728–740.

Boose, E., & Gould, E. (2019). *Harvard Forest Climate Data since 1964*.

Boyer, J. S. (1968). Relationship of water potential to growth of leaves. *Plant Physiology*, *43*, 1056–1062.

Buttò, V., Deslauriers, A., Rossi, S., Rozenberg, P., Shishov, V., & Morin, H. (2020). The role of plant hormones in tree-ring formation. *Trees*, *34*, 315–335.

Cabon, A., Fernández-de-Uña, L., Gea-Izquierdo, G., Meinzer, F. C., Woodruff, D. R., Martínez-Vilalta, J., & Cáceres, M. D. (2020). Water potential control of turgor-driven tracheid enlargement in scots pine at its xeric distribution edge. *New Phytologist*, *225*, 209–221.

Cabon, A., Peters, R. L., Fonti, P., Martínez-Vilalta, J., & Cáceres, M. D. (2020). Temperature and water potential co-limit stem cambial activity along a steep elevational gradient. *New Phytologist*, *226*, 1325–1340.

Carbone, M. S., Czimczik, C. I., Keenan, T. F., Murakami, P. F., Pederson, N., Schaberg, P. G., … Richardson, A. D. (2013). Age, allocation and availability of nonstructural carbon in mature red maple trees. *New Phytologist*, *200*, 1145–1155.

Carbone, M. S., Seyednasrollah, B., Rademacher, T. T., Basler, D., Le Moine, J. M., Beals, S., … Richardson, A. D. (2019). Flux puppy–An open-source software application and portable system design for low-cost manual measurements of CO2 and H2O fluxes. *Agricultural and Forest Meteorology*, *274*, 1–6.

Cartenì, F., Deslauriers, A., Rossi, S., Morin, H., De Micco, V., Mazzoleni, S., & Giannino, F. (2018). The physiological mechanisms behind the Earlywood-to-latewood transition: A process-based modeling approach. *Frontiers in Plant Science*, *9*, 1053.

Castagneri, D., Prendin, A. L., Peters, R. L., Carrer, M., von Arx, G., & Fonti, P. (2020). Long-Term Impacts of Defoliator Outbreaks on Larch Xylem Structure and Tree-Ring Biomass. *Frontiers in Plant Science*, *11*. http://dx.doi.org/10.3389/fpls.2020.01078.

Chow, P. S., & Landhausser, S. M. (2004). A method for routine measurements of total sugar and starch content in woody plant tissues. *Tree Physiology*, *24*, 1129–1136.

Cuny, H. E., Fonti, P., Rathgeber, C. B. K., von Arx, G., Peters, R. L., & Frank, D. C. (2018). Couplings in cell differentiation kinetics mitigate air temperature influence on conifer wood anatomy. *Plant, Cell & Environment*, *42*, 1222–1232.

Cuny, H. E., & Rathgeber, C. B. K. (2016). Xylogenesis: Coniferous trees of temperate forests are listening to the climate tale during the growing season but only remember the last words! *Plant Physiology*, *171*, 306–317.

Cuny, H. E., Rathgeber, C. B. K., Frank, D., Fonti, P., Mäkinen, H., Prislan, P., … Fournier, M. (2015). Woody biomass production lags stem-girth increase by over one month in coniferous forests. *Nature Plants*, *1*(11). http://dx.doi.org/10.1038/nplants.2015.160.

Daudet, F.-A. (2004). Experimental analysis of the role of water and carbon in tree stem diameter variations. *Journal of Experimental Botany*, *56*, 135–144.

De Schepper, V., & Steppe, K. (2011). Tree girdling responses simulated by a water and carbon transport model. *Annals of Botany*, *108*, 1147–1154.

De Schepper, V., Vanhaecke, L., & Steppe, K. (2011). Localized stem chilling alters carbon processes in the adjacent stem and in source leaves. *Tree Physiology*, *31*, 1194–1203.

Deslauriers, A., Caron, L., & Rossi, S. (2015). Carbon allocation during defoliation: testing a defense-growth trade-off in balsam fir. *Frontiers in Plant Science*, *6*. http://dx.doi.org/10.3389/fpls.2015.00338.

Domec, J.-C., & Pruyn, M. L. (2008). Bole girdling affects metabolic properties and root, trunk and branch hydraulics of young ponderosa pine trees. *Tree Physiology*, *28*, 1493–1504.

Fatichi, S., Leuzinger, S., & Körner, C. (2014). Moving beyond photosynthesis: From carbon source to sink-driven vegetation modeling. *New Phytologist*, *201*, 1086–1095.

Fierravanti, A., Rossi, S., Kneeshaw, D., De Grandpré, L., & Deslauriers, A. (2019). Low non-structural carbon accumulation in spring reduces growth and increases mortality in conifers defoliated by spruce budworm. *Frontiers in Forests and Global Change*, *2*, 15.

Friend, A. D., Eckes-Shephard, A. H., Fonti, P., Rademacher, T. T., Rathgeber, C. B. K., Richardson, A. D., & Turton, R. H. (2019). On the need to consider wood formation processes in global vegetation models and a suggested approach. *Annals of Forest Science*, *76*, 49.

Friend, A. D., Lucht, W., Rademacher, T. T., Keribin, R., Betts, R., Cadule, P., … Woodward, F. I. (2014). Carbon residence time dominates uncertainty in terrestrial vegetation responses to future climate and atmospheric CO $_2$. *Proceedings of the National Academy of Sciences*, *111*, 3280–3285.

Furze, M. E., Huggett, B. A., Aubrecht, D. M., Stolz, C. D., Carbone, M. S., & Richardson, A. D. (2019). Whole-tree nonstructural carbohydrate storage and seasonal dynamics in five temperate species. *New Phytologist*, *221*, 1466–1477.

Furze, M. E., Huggett, B. A., Chamberlain, C. J., Wieringa, M. M., Aubrecht, D. M., Carbone, M. S., … Richardson, A. D. (2020). Seasonal fluctuation of nonstructural carbohydrates reveals the metabolic availability of stemwood reserves in temperate trees with contrasting wood anatomy. *Tree Physiology*, *40*, 1355–1365.

Galbraith, D., Malhi, Y., Affum-Baffoe, K., Castanho, A. D. A., Doughty, C. E., Fisher, R. A., … Lloyd, J. (2013). Residence times of woody biomass in tropical forests. *Plant Ecology & Diversity*, *6*, 139–157.

Gessler, A., & Grossiord, C. (2019). Coordinating supply and demand: Plant carbon allocation strategy ensuring survival in the long run. *New Phytologist*, *222*, 5–7.

Gould, G. W., Measures, J. C., Wilkie, D. R., Meares, P., Richards, R. E., & Franks, F. (1977). Water relations in single cells. *Philosophical transactions of the Royal Society of London. B, Biological Sciences*, *278*, 151–166.

Guerriero, G., Sergeant, K., & Hausman, J.-F. (2014). Wood biosynthesis and typologies: A molecular rhapsody. *Tree Physiology*, *34*, 839–855.

Hagedorn, F., Joseph, J., Peter, M., Luster, J., Pritsch, K., Geppert, U., … Arend, M. (2016). Recovery of trees from drought depends on belowground sink control. *Nature Plants*, *2*(8). http://dx.doi.org/10.1038/nplants.2016.111.

Hartmann, H., Adams, H. D., Hammond, W. M., Hoch, G., Landhäusser, S. M., Wiley, E., & Zaehle, S. (2018). Identifying differences in carbohydrate dynamics of seedlings and mature trees to improve carbon allocation in models for trees and forests. *Environmental and Experimental Botany*, *152*, 7–18.

Hartmann, H., Bahn, M., Carbone, M., & Richardson, A. D. (2020). Plant carbon allocation in a changing world–Challenges and progress: Introduction to a virtual issue on carbon allocation. *New Phytologist*, *227*, 981–988.

Hartmann, H., McDowell, N. G., & Trumbore, S. (2015). Allocation to carbon storage pools in Norway spruce saplings under drought and low CO2. *Tree Physiology*, *35*, 243–252.

Hayat, A., Hacket-Pain, A. J., Pretzsch, H., Rademacher, T. T., & Friend, A. D. (2017). Modeling Tree Growth Taking into Account Carbon Source and Sink Limitations. *Frontiers in Plant Science*, *8*. http://dx.doi.org/10.3389/fpls.2017.00182.

Henriksson, N., & Rademacher, T. T. (2019). Stem compression: A means to reversibly reduce phloem transport in tree stems. In J. Liesche (Ed.), *Methods in molecular biology*. *Phloem: Methods and protocols* (pp. 301–310). New York, NY: Springer.

Henriksson, N., Tarvainen, L., Lim, H., Tor-Ngern, P., Palmroth, S., Oren, R., … Näsholm, T. (2015). Stem compression reversibly reduces phloem transport in *Pinus sylvestris* trees. *Tree Physiology*, *35*, 1075–1085.

Hsiao, T. C., Acevedo, E., Fereres, E., Henderson, D. W., Monteith, J. L., & Weatherley, P. E. (1976). Water stress, growth and osmotic adjustment. *Philosophical transactions of the Royal Society of London. B, Biological Sciences*, *273*, 479–500.

Huang, J., Hammerbacher, A., Weinhold, A., Reichelt, M., Gleixner, G., Behrendt, T., … Hartmann, H. (2019). Eyes on the future–Evidence for trade-offs between growth, storage and defense in Norway spruce. *New Phytologist*, *222*, 144–158.

Jordan, M.-O., & Habib, R. (1996). Mobilizable carbon reserves in young peach trees as evidenced by trunk girdling experiments. *Journal of Experimental Botany*, *47*, 79–87.

Körner, C. (2003). Carbon limitation in trees. *Journal of Ecology*, *91*, 4–17.

Körner, C., Asshoff, R., Bignucolo, O., Hättenschwiler, S., Keel, S. G., Peláez-Riedl, S., … Zotz, G. (2005). Carbon flux and growth in mature deciduous Forest trees exposed to elevated CO_2. *Science*, *309*, 1360–1362.

Lamlom, S. H., & Savidge, R. A. (2003). A reassessment of carbon content in wood: Variation within and between 41 north American species. *Biomass and Bioenergy*, *25*, 381–388.

Lastdrager, J., Hanson, J., & Smeekens, S. (2014). Sugar signals and the control of plant growth and development. *Journal of Experimental Botany*, *65*, 799–807.

Maier, C. A., Johnsen, K. H., Clinton, B. D., & Ludovici, K. H. (2010). Relationships between stem CO2 efflux, substrate supply, and growth in young loblolly pine trees. *New Phytologist*, *185*, 502–513.

Maunoury-Danger, F., Fresneau, C., Eglin, T., Berveiller, D., Francois, C., Lelarge-Trouverie, C., & Damesin, C. (2010). Impact of carbohydrate supply on stem growth, wood and respired CO_2 ^{13}C: Assessment by experimental girdling. *Tree Physiology*, *30*, 818–830.

Minchin, P. E. H., & Lacointe, A. (2005). New understanding on phloem physiology and possible consequences for modelling long-distance carbon transport. *New Phytologist*, *166*, 771–779.

Moscatello, S., Proietti, S., Augusti, A., Scartazza, A., Walker, R. P., Famiani, F., & Battistelli, A. (2017). Late summer photosynthesis and storage carbohydrates in walnut (*Juglans regia* L.): Feed-back and feed-forward effects. *Plant Physiology and Biochemistry*, *118*, 618–626.

Muhr, J., Trumbore, S., Higuchi, N., & Kunert, N. (2018). Living on borrowed time-Amazonian trees use decade-old storage carbon to survive for months after complete stem girdling. *New Phytologist*, *220*, 111–120.

Nikinmaa, E., Sievänen, R., & Hölttä, T. (2014). Dynamics of leaf gas exchange, xylem and phloem transport, water potential and carbohydrate concentration in a realistic 3-D model tree crown. *Annals of Botany*, *114*, 653–666.

Niklas, K. J. (1992). *Plant biomechanics: An engineering approach to plant form and function*. Chicago, IL: University of Chicago Press.

Oberhuber, W., Gruber, A., Lethaus, G., Winkler, A., & Wieser, G. (2017). Stem girdling indicates prioritized carbon allocation to the root system at the expense of radial stem growth in Norway spruce under drought conditions. *Environmental and Experimental Botany*, *138*, 109–118.

Pan, Y., Birdsey, R. A., Fang, J., Houghton, R., Kauppi, P. E., Kurz, W. A., … Hayes, D. (2011). A large and persistent carbon sink in the World's forests. *Science*, *333*, 988–993.

Perez-Priego, O., Guan, J., Rossini, M., Fava, F., Wutzler, T., Moreno, G., … Migliavacca, M. (2015). Sun-induced chlorophyll fluorescence and photochemical reflectance index improve remote-sensing gross primary production estimates under varying nutrient availability in a typical Mediterranean savanna ecosystem. *Biogeosciences*, *12*, 6351–6367.

Peters, R. L., Steppe, K., Cuny, H. E., De Pauw, D. J. W., Frank, D. C., Schaub, M., … Fonti, P. (2021). Turgor—A limiting factor for radial growth in mature conifers along an elevational gradient. *New Phytologist*, *229*, 213–229.

Piper, F. I., Gundale, M. J., & Fajardo, A. (2015). Extreme defoliation reduces tree growth but not C and N storage in a winter-deciduous species. *Annals of Botany*, *115*, 1093–1103.

Pugh, T. A. M., Rademacher, T. T., Shafer, S. L., Steinkamp, J., Barichivich, J., Beckage, B., … Thonicke, K. (2020). Understanding the uncertainty in global forest carbon turnover. *Biogeosciences Discussions*, *17*, 1–44. https://doi.org/10.5194/bg-2019-491.

R Core Team. (2019). *R: A language and environment for statistical computing*. Vienna, Austria: R Foundation for Statistical Computing.

Rademacher, T., & Richardson, A. D. (2020). *White pine girdling and compression experiment at Harvard Forest 2017–2019*. Harvard Forest Data Archive. https://doi.org/10.6073/pasta/f0807db4a0cea409aee065fe21d940da

Rademacher, T., Seyednasrollah, B., Basler, D., Cheng, J., Mandra, T., & Richardson, A. D. (2020). The Wood Image Analysis and Dataset (WIAD): Open-access visual analysis tools to advance the ecological data revolution. *bioRxiv*. https://harvardforest1.fas.harvard.edu/exist/apps/datasets/showData.html?id=hf348.

Rademacher, T. T., Basler, D., Eckes-Shephard, A. H., Fonti, P., Friend, A. D., Le Moine, J., & Richardson, A. D. (2019). Using direct phloem transport manipulation to advance understanding of carbon dynamics in Forest trees. *Frontiers in Forests and Global Change*, *2*.

Rathgeber, C. B. K., Cuny, H. E., & Fonti, P. (2016). Biological basis of tree-ring formation: A crash course. *Frontiers in Plant Science*, *7*.

Regier, N., Streb, S., Zeeman, S. C., & Frey, B. (2010). Seasonal changes in starch and sugar content of poplar (*Populus deltoides* x nigra cv. Dorskamp) and the impact of stem girdling on carbohydrate allocation to roots. *Tree Physiology*, *30*, 979–987.

Richardson, A. D., Carbone, M. S., Huggett, B. A., Furze, M. E., Czimczik, C. I., Walker, J. C., … Murakami, P. (2015). Distribution and mixing of old and new nonstructural carbon in two temperate trees. *New Phytologist*, *206*, 590–597.

Riou-Khamlichi, C., Menges, M., Healy, J. M. S., & Murray, J. A. H. (2000). Sugar control of the plant cell cycle: Differential regulation of Arabidopsis D-type Cyclin gene expression. *Molecular and Cellular Biology*, *20*, 4513–4521.

Rossi, S., Anfodillo, T., & Menardi, R. (2006). Trephor: A new tool for sampling microcores from tree stems. *IAWA Journal*, *27*, 89–97.

Rossi, S., Deslauriers, A., Anfodillo, T., Morin, H., Saracino, A., Motta, R., & Borghetti, M. (2006). Conifers in cold environments synchronize maximum growth rate of tree-ring formation with day length. *New Phytologist*, *170*, 301–310.

Rossi, S., Simard, S., Deslauriers, A., & Morin, H. (2009). Wood formation in *Abies balsamea* seedlings subjected to artificial defoliation. *Tree Physiology*, *29*, 551–558.

Salmon, Y., Lintunen, A., Dayet, A., Chan, T., Dewar, R., Vesala, T., & Hölttä, T. (2020). Leaf carbon and water status control stomatal and nonstomatal limitations of photosynthesis in trees. *New Phytologist*, *226*, 690–703.

Smith, A. M., & Stitt, M. (2007). Coordination of carbon supply and plant growth. *Plant, Cell & Environment*, *30*, 1126–1149.

Sovonick-Dunford, S., Lee, D. R., & Zimmermann, M. H. (1981). Direct and indirect measurements of phloem turgor pressure in white ash. *Plant Physiology*, *68*, 121–126.

Sperry, J. S. (2003). Evolution of water transport and xylem structure. *International Journal of Plant Sciences*, *164*, S115–S127.

Steppe, K., Sterck, F., & Deslauriers, A. (2015). Diel growth dynamics in tree stems: Linking anatomy and ecophysiology. *Trends in Plant Science*, *20*, 335–343.

Tyree, M. T., & Zimmermann, M. H. (2002). *Xylem structure and the ascent of sap*. Berlin Heidelberg: Springer-Verlag.

Uggla, C., Magel, E., Moritz, T., & Sundberg, B. (2001). Function and dynamics of Auxin and carbohydrates during Earlywood/latewood transition in scots pine. *Plant Physiology*, *125*, 2029–2039.

van der Sleen, P., Groenendijk, P., Vlam, M., Anten, N. P. R., Boom, A., Bongers, F., … Zuidema, P. A. (2015). No growth stimulation of tropical trees by 150 years of CO2 fertilization but water-use efficiency increased. *Nature Geoscience*, *8*, 24–28.

Vargas, R., Trumbore, S. E., & Allen, M. F. (2009). Evidence of old carbon used to grow new fine roots in a tropical forest. *New Phytologist*, *182*, 710–718.

Vieira, J., Carvalho, A., & Campelo, F. (2020). Tree growth under climate change: Evidence from Xylogenesis timings and kinetics. *Frontiers in Plant Science*, *11*.

Voelker, S. L., Muzika, R.-M., Guyette, R. P., & Stambaugh, M. C. (2006). Historical CO_2 growth Engancement declines with age in *Quercus* and *Pinus*. *Ecological Monographs*, *76*, 549–564.

von Arx, G., & Carrer, M. (2014). ROXAS–A new tool to build centuries-long tracheid-lumen chronologies in conifers. *Dendrochronologia*, *32*, 290–293.

Walker, A. P., De Kauwe, M. G., Bastos, A., Belmecheri, S., Georgiou, K., Keeling, R. F., … Zuidema, P. A. (2021). Integrating the evidence for a terrestrial carbon sink caused by increasing atmospheric CO 2. *New Phytologist*, *229*(5), 2413–2445. http://dx.doi.org/10.1111/nph.16866.

Weber, R., Gessler, A., & Hoch, G. (2019). High carbon storage in carbon-limited trees. *New Phytologist*, *222*, 171–182.

Wiley, E., Casper, B. B., & Helliker, B. R. (2017). Recovery following defoliation involves shifts in allocation that favour storage and reproduction over radial growth in black oak. *Journal of Ecology*, *105*, 412–424.

Wilson, B. F. (1968). Effect of girdling on cambial activity in white pine. *Canadian Journal of Botany*, *46*, 141–146.

Winkler, A., & Oberhuber, W. (2017). Cambial response of Norway spruce to modified carbon availability by phloem girdling. *Tree Physiology*, *37*, 1527–1535.

Wright, J. P., & Fisher, D. B. (1980). Direct measurement of sieve tube turgor pressure using severed aphid stylets. *Plant Physiology*, *65*, 1133–1135.

Zhang, J., Alexander, M. R., Gou, X., Deslauriers, A., Fonti, P., Zhang, F., & Pederson, N. (2020). Extended xylogenesis and stem biomass production in Juniperus przewalskii Kom. During extreme late-season climatic events. *Annals of Forest Science*, *77*, 99.

Zhang, P., Zhou, X., Fu, Y., Shao, J., Zhou, L., Li, S., … McDowell, N. G. (2020). Differential effects of drought on nonstructural carbohydrate storage in seedlings and mature trees of four species in a subtropical forest. *Forest Ecology and Management*, *469*, 118159.

SUPPORTING INFORMATION

Additional supporting information may be found online in the Supporting Information section at the end of this article.

How to cite this article: Rademacher, T., Fonti, P., LeMoine, J. M., Fonti, M. V., Basler, D., Chen, Y., Friend, A. D., Seyednasrollah, B., Eckes-Shephard, A. H., & Richardson, A. D. (2021). Manipulating phloem transport affects wood formation but not local nonstructural carbon reserves in an evergreen conifer. *Plant, Cell & Environment*, *44*(8), 2506–2521. https://doi.org/10.1111/pce.14117